



Anal. Bioanal. Chem. Res., Vol. 11, No. 3, 281-290, July 2024.

Electrochemical Analysis of Caffeine at the Electrode Modified by Functionalized Graphene Oxide with Alizarin Red

Roya Sepehri Pour^a, Mohammad Mazloun-Ardakani^{a,*} and Mohammad Ali Sheikh Mohseni^b

^a*Department of Chemistry, Faculty of Science, Yazd University, Yazd, I.R. Iran*

^b*Shahid Bakeri Higher Education Center of Miandoab, Urmia University, Urmia, I.R. Iran*

(Received 16 October 2023, Accepted 10 March 2024)

In this study, reduced graphene oxide (RGO) was first synthesized and then it was reacted by alizarin red S (ARS), and therefore RGO functionalized with ARS was prepared (ARS/RGO). Then, structural analysis of the manufactured material was done by SEM and FTIR techniques. The FTIR results confirmed the interaction between ARS and RGO and the formation of ARS/RGO. A new electrochemical sensor was fabricated on the surface of a glassy carbon electrode modified with ARS/RGO. The prepared electrode showed a quasi-reversible electrochemical behavior and also had a significant effect on the electrocatalytic oxidation of caffeine (CAF). The modified electrode was able to measure the CAF as an electrochemical sensor. The effect of different parameters was investigated on the oxidation of CAF at the modified electrode; the sensor has the highest current at pH = 4.0. The effect of different interference species on the response of CAF, and also the reproducibility and repeatability of the sensor was investigated and acceptable results were obtained. The electrochemical determination of CAF on the electrode surface was investigated by differential pulse voltammetry and in the linear range of 1.0-100.0 μM , the detection limit value was obtained as 0.022 μM . Finally, the designed sensor was used to measure the amount of CAF in some real samples and satisfactory results were obtained.

Keywords: Voltammetry, Nanomaterials, Electroanalysis, Sensor

INTRODUCTION

Caffeine (CAF) is a xanthine alkaloid compound (1,3,7-trimethylxanthine), and its molecular shape is similar to that of adenosine. Adenosine is a neuromodulator that inhibits the central nervous system. As a result of adenosine binding to its receptors, it prevents the release of some neurotransmitters, which ultimately produces an anticonvulsant with a sedative effect [1]. Due to the similarity of the molecular shape of CAF to adenosine, adenosine receptors bind to CAF molecules and reduce the effect of adenosine on its receptors, thereby preventing sleepiness caused by adenosine [2]. In addition to stimulating the central nervous system, it boosts mental function and concentration

and relieves fatigue. Also exerts positive effects on the body and contributes to the prevention of several diseases [3]. The European Committee of Experts on Food Science has recommended a daily CAF intake of less than 400 mg for adults [4]. Excessive consumption of caffeine can provoke health disorders, such as irregular heartbeat, upset stomach, trembling hands, restlessness, diminished memory, asthma, and sleeping difficulty [5].

Therefore, it is necessary to determine the CAF content in beverages and other related sources. Different methods have been developed for the determination of CAF such as fluorescence [6,7], high-performance liquid chromatography [8,9], ultra-performance liquid chromatography (UPLC) with UV detection (HPLC) [10], capillary electrophoresis (CE) [11], gas chromatography with flame ionization detection (GC-FID) [12], thin layer chromatography [13]. Also, there

*Corresponding author. E-mail: mazloun@yazd.ac.ir

are various studies in the field of spectrophotometric monitoring of the kinetics of caffeine that reacts with oxidant agents [13-15]. In general, these methods are time-consuming, complicated, and costly. Instead, electrochemical methods can be used for the determination of CAF and have advantages such as fast, high sensitivity, good stability, and repeatability, requiring few sample preparations and being relatively inexpensive [16-18].

Some factors such as the electrode and its surface play an important role in increasing the efficiency of the electrochemical method [19-21]. Different materials can be used to develop electrochemical sensors, these include ionic liquids, macrocycle compounds (cyclodextrin), metal complexes (phthalocyanines and porphyrins), carbon materials (graphene and nanotube), and metal nanoparticles [22-24]. According to the studies conducted in the construction of sensors, the use of carbon materials together with organic compounds creates a synergistic effect between the materials, which leads to the production of very sensitive sensing platforms for the detection of the desired analyte. In these cases, the organic materials with redox activity interact with the analyte and the carbon materials accelerate the electron transfer [25]. In most reported works in this field, the carbon nanomaterial and the organic compound were mixed simply at the surface or bulk of the electrode [26,27]. Rarely, the carbon nanomaterial has been functionalized by the organic compound and then has been used in the modified electrodes [28]. Among carbon nanomaterials, graphene oxide has received much attention due to its properties such as mechanical strength, and thermal and electrical conductivity, as well as having carboxyl, hydroxy, and epoxy groups that provide a favorable substrate for the functionalization of molecules [29]. Different methods can be used to change the physical and chemical properties of carbon nanomaterials including functionalizing their side chain with appropriate functional groups. This process is due to the formation of covalent bonds or physical surface absorption [30-32]. Among these methods, the most preferred method is physical surface absorption, because this method does not change the primary structure of the carbon nanomaterials [30].

Sodium 1,2-dihydroxytetraquinone-3-sulfonic acid (alizarin red S) (ARS), is known as a complexing agent involved in the photometric determination of small amounts

of analyts [33]. Also as an electroactive species and a surface active compound, it can be reversibly reduced to anthrahydroquinone. Therefore, this organic compound is an appropriate choice for electrocatalytic electrochemical sensors [34,35]. The electrochemical properties of ARS can be improved by the simultaneous use of ARS and carbon nanotubes in modified electrodes [36]. But the functionalizing of graphene oxide by ARS or other types of interaction of ARS with carbon nanomaterials was not studied completely yet. According to some research, the carbon nanotubes can be functionalized with ARS through Non-covalent interactions [37].

In this paper, we report an electrochemical sensor for CAF. This sensor work based on the synergistic effect of graphene and ARS. The graphene was functionalized by ARS with a simple physical surface absorption process. We investigate the electrocatalytic oxidation of caffeine with a mixture of ARS and RGO on the designed glassy carbon electrode. To the best of our knowledge, determination of CAF using ARS/RGO composite modified electrode has not been reported.

MATERIALS AND METHODS

Reagents and Apparatus

Alizarin Red S, sodium hydroxide, phosphoric acid (85%), sulfuric acid (98%), glutamic acid, tryptophan, glycine, cysteine, alumina powder, graphite powder, nitric acid, acetic acid, hydrogen peroxide (30%), potassium permanganate (99%) and hydrogen chloride (37%) from Merck (Darmstadt, Germany), potassium chloride (99.5%), caffeine (99%) and glucose (99.5%) were obtained from Sigma-Aldrich (Steinheim, Germany). No additional purification was done on the material.

Electrochemical measurements were carried out using Ivium's potentiostat-galvanostat device (model IviumStat,h, the Netherlands) and equipped with an electrochemical cell containing three electrodes. The electrodes include the platinum wire electrode as the counter electrode, Ag/AgCl/sat.KCl electrode as the reference electrode and glassy carbon electrode ($A = 0.0314 \text{ cm}^2$, Azar Electrode, Urmia, Iran) as the working electrode. The pH measurement was made by a Metrohm pH meter, model 691. All solutions were freshly prepared with double distilled water. The RGO

used in this study was synthesized based on our previously reported method [38].

Preparation of Modified Electrode

The alizarin red S/graphene oxide composite was made by mixing solutions of them with different concentrations and different solvents. In optimum conditions, a 1.0 mg ml⁻¹ solution of graphene oxide and 0.1 mg ml⁻¹ solution of ARS were combined, and then the resulting mixture was stirred for 2 h at room temperature. This mixture was used as a modifier for the following step.

To prepare the modified glassy carbon electrode, first, the surface of the electrode was polished with alumina slurry on a cloth with a diagonal texture. Then, to remove alumina particles from the electrode, its surface was washed twice with distilled water. After washing the electrode surface, the electrode was immersed in 1.0 M sulfuric acid solution for 1 min. Then it was washed again with distilled water and allowed to dry. After that, 0.2 µl of modifier (*i.e.* ARS/RGO) solution was applied dropwise on the electrode surface. Then the electrode was dried for 30 min at room temperature. The resulting electrode was called ARS/RGO-GCE.

Preparation of Real Sample

Samples of commercially available black tea, coffee, and chocolate milk were purchased from a local supermarket and analyzed shortly after opening. Solid samples (black tea and coffee) taken from five packages of the same brand were previously mixed in a mortar. An accurately weighed portion of coffee powder was dispersed in 25 ml of water/ethanol mixture (50:50 v/v) and then left in an ultrasonic bath for 30 min. For the black tea sample, an accurately weighed portion was infused in boiled water for about 15 min. In the case of the chocolate milk sample, the content of three bottles was mixed thoroughly, and sonicated to remove CO₂. Finally, a suitable volume of the resulting solutions of each sample was transferred to a voltammetric cell and reached the desired volume by phosphate buffer solution, pH 4.0, and then analyzed.

RESULTS AND DISCUSSION

Characterization of the Modifier

The synthesized graphene oxide was examined by scanning electron microscope and the resulting image is

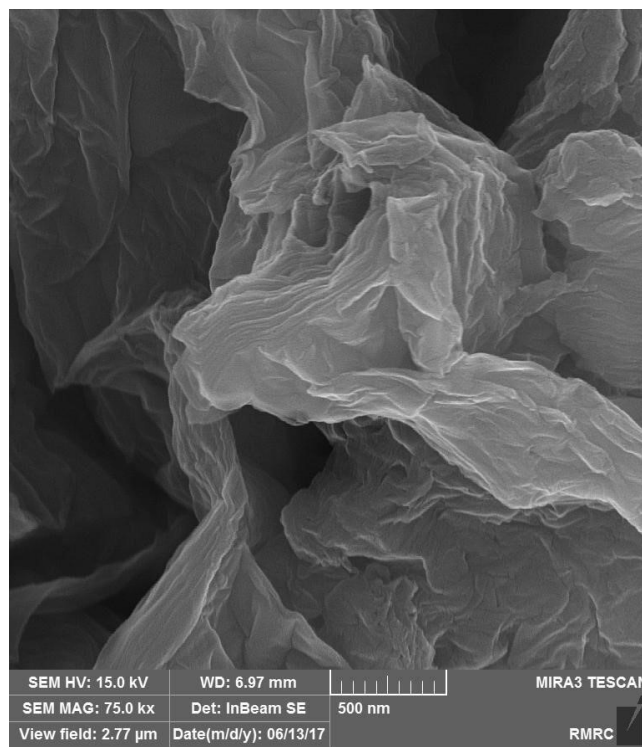


Fig. 1. SEM image of synthesized graphene oxide nanosheets.

shown in Fig. 1. According to the image, the graphene oxide sheets are like thin paper with smooth surfaces, along with wrinkles.

The modifier (alizarin red S/graphene oxide composite or ARS/RGO) has been characterized by FT-IR (Fig. 2). In this figure, part (a), (b) and (c) respectively show the FTIR spectrums of RGO, ARS and ARS/RGO. In the case of RGO (Fig. 2a, there is a stretching C-O band at 1222 cm⁻¹, a broad COOH band at 2500-3500 cm⁻¹, a stretching OH band at 3300-3500 cm⁻¹ and a stretching C=O band at 1690-1720 cm⁻¹, which indicates the correct structure of graphene oxide [39]. In the FT-IR spectrum of ARS in Fig. 2b, the 1184 cm⁻¹ band represents the C-C band, 1261 the cm⁻¹ band represents the C-O band, the 1486 cm⁻¹ band, and the 1587 cm⁻¹ band represent C=C stretching, the 1632 cm⁻¹ band represents the C=O band and the 3391 cm⁻¹ band represents the stretching OH [40]. In part (c), which shows the FT-IR spectrum of ARS/RGO, the characterizations of the FT-IR spectrum of both RGO and ARS can be seen. When alizarin molecules are attached to the graphene surface, characteristic

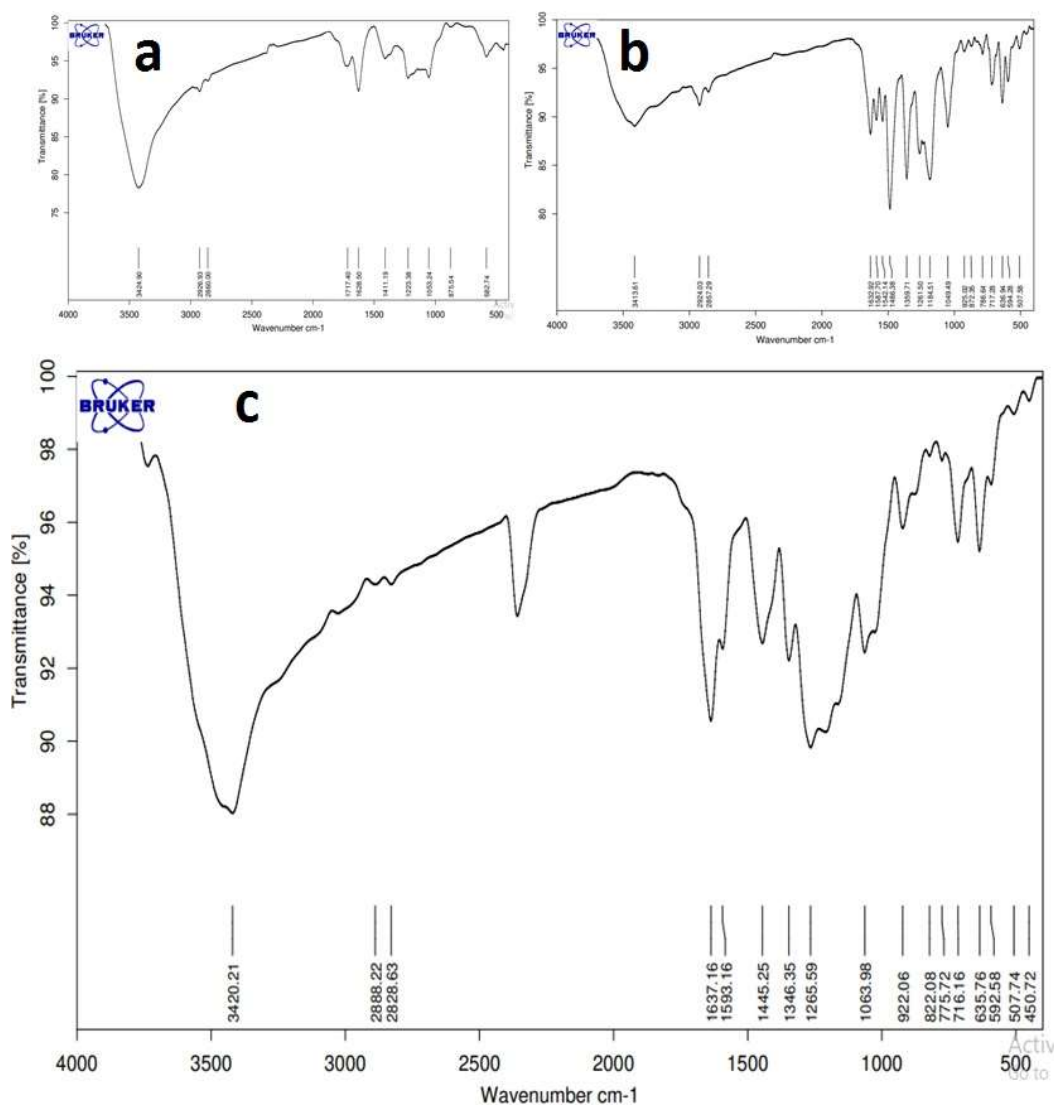


Fig. 2. FT-IR spectrum of (a) synthesized RGO (b) ARS (c) ARS/RGO.

peaks corresponding to the functional groups of alizarin can be observed in the FTIR spectrum. Therefore, the ARS/RGO was synthesized successfully and graphene oxide was functionalized by ARS.

Electrochemical Behavior of ARS/RGO-GCE

To investigate the electrochemical behavior of the modified electrode, ARS/RGO-GCE, first the electrode was placed in a 0.1 M phosphate buffer solution with a pH of 4.0, and then its electrochemical behavior was determined using the cyclic voltammetry method. The anodic peak potential is

0.68 V and the cathodic peak potential is 0.59 V (Fig. 3, curve (c)). The peak separation (ΔE_p) for this system is about 0.09 V, which indicates the quasi-reversible behavior of the ARS/RGO on the glassy carbon electrode surface. The cyclic voltammograms of RGO-GCE and ARS-GCE were also recorded (Fig. 3 curves (a) and (b), respectively). As can be seen, the ARS has no suitable cyclic voltammetry response and just a broad anodic irreversible peak was obtained at the conditions. Therefore, the combination of ARS and RGO in ARS/RGO can enhance the electrochemical behavior of ARS. The improved electron transfer from the RGO sheets to

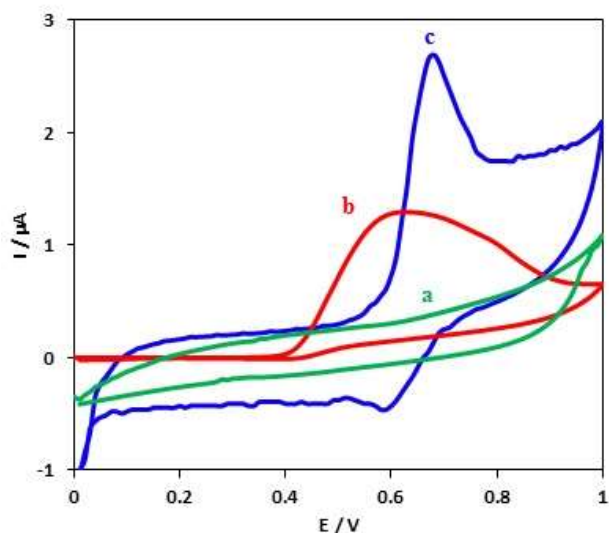


Fig. 3. Cyclic voltammograms of (a) RGO-GCE, (b) ARS-GCE, and (c) ARS/RGO-GCE (RGO = 1.0 mg ml⁻¹ and ARS = 0.1 mg ml⁻¹) in 0.1 M phosphate buffer solution with pH = 4.0; potential scan rate is 50.0 mV s⁻¹.

their linked ARS is responsible for the electrochemical behavior of ARS/RGO-GCE.

Figure 4a shows the influence of potential scan rate on the cyclic voltammetry responses of the ARS/RGO-GCE in 0.1 M phosphate buffer solution with pH = 4.0. The anodic and also cathodic peak currents were linearly proportional to the scan rate in the range from 15.0 to 1000.0 mV s⁻¹ (Fig. 4b), and it shows that the oxidation/reduction process of ARS/RGO on the electrode surface is a surface-dependent process, in other words, the existence of a linear relationship indicates the stabilization of the modifier on the surface of the glassy carbon electrode and the process is not under diffusion control [41]. By the slope of those curves and the Sharp equation and assuming that the electrochemical process is two-electron and the surface area of the electrode is 0.0314 cm², the amount of surface coverage is calculated as $\Gamma = 2.3 \times 10^{-10}$ mol cm⁻² [41].

The separation of anodic and cathodic peak potentials to the scan rate of 175 mV s⁻¹ is low; therefore the ARS/RGO has high kinetic charge transfer below this scan rate (Fig. 4c). Figure 4d shows the plot of the anodic and cathodic peak potentials of ARS/RGO-GCE *versus* the logarithm of the potential scan rate at scan rates above 175 mV s⁻¹. By the

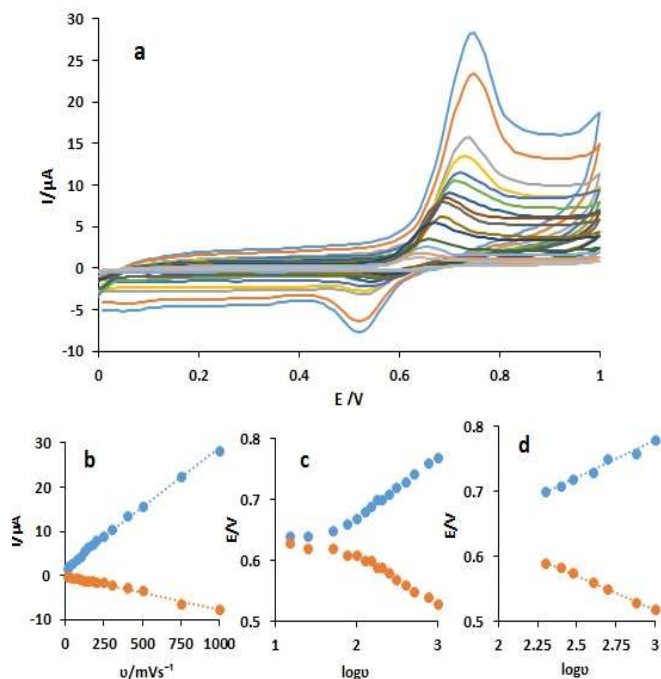


Fig. 4. (a) Cyclic voltammograms of ARS/RGO-GCE in 0.1 M phosphate buffer solution (pH = 4.0) for different scan rates from inner to outer: 15, 25, 50, 75, 100, 125, 150, 200, 250, 300, 400, 500, 750 and 1000 mV s⁻¹; (b) variations of cathodic and anodic peak current vs. potential scan rate; (c) anodic and cathodic peak potential vs. the logarithm of potential scan rate (d) anodic and cathodic peak potential *versus* the logarithm of the scan rate for above 175 mV s⁻¹.

slope of these plots and considering $n_a = 1$, the value of oxidation and reduction transfer coefficients of ARS/RGO-GCE was calculated as 0.6 and 0.4, respectively. Also, according to the theory of Laviron, the average value of the apparent transfer rate constant was calculated as 2.64 s⁻¹ [42].

Electrocatalysis of Caffeine on the ARS/RGO-GCE

The oxidation of CAF was studied at the surface of different modified electrodes in a 0.1 M phosphate buffer solution (pH 4.0) containing 100.0 μM CAF. The obtained cyclic voltammograms at the bare GCE (curve a), RGO-GCE (curve b), ARS-GCE (curve c), and ARS/RGO-GCE (curve d) are shown in Fig. 5. Any anodic or cathodic peak was not observed at the bare GCE (curve a). At the RGO-GCE there was a little increase in background current and the

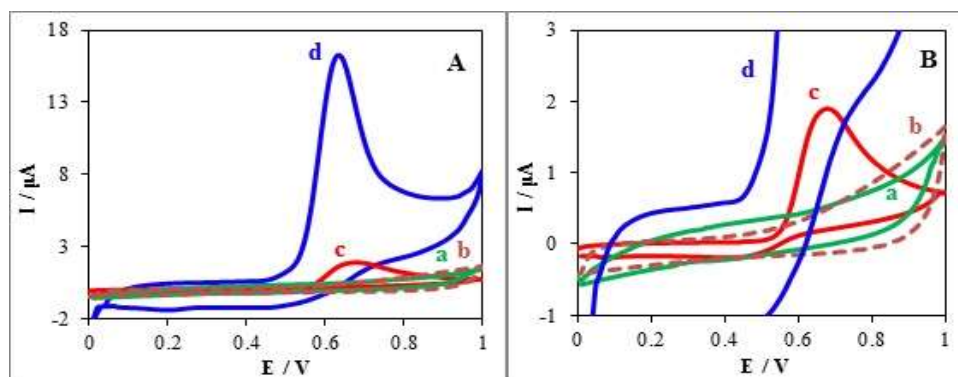


Fig. 5. Cyclic voltammograms of 100.0 μM CAF at the bare GCE (curve a), RGO-GCE (curve b), ARS-GCE (curve c) and ARS/RGO-GCE (curve d) in a 0.1 M phosphate buffer solution (pH 4.0), scan rate is 50 mV s^{-1} ; parts (A) and (B) are same but part (B) is magnified.

CAF was not oxidized similar to bare GCE (curves a and b). By modifying the electrode with ARS, the CAF can be oxidized at ARS-GCE and the anodic peak current of ARS was increased (curve c). But the best oxidation of CAF occurred at the modified electrode with ARS/RGO which a high anodic current, *i.e.* $16 \mu\text{A}$, was obtained (curve d). The presence of ARS on the RGO nanosheets, besides the increasing the surface area of the electrode and more availability of the ARS, causes better electron transfer from RGO to ARS and. Therefore the CAF can be oxidized better by the oxidized form of ARS through EC' mechanism. This mechanism is shown in Fig. 6. As can be seen, the ARS first oxidized at the electrode surface and then oxidized forms of ARS oxidize the CAF and convert to the initial form.

Effect of pH on Electrocatalytic Oxidation of Caffeine

The peak potential and peak current of CAF are related to the pH of the electrolyte solution. The effect of pH on the electrochemical response of CAF at the ARS/RGO-GCE surface was investigated in a phosphate buffer solution with different pHs in the range of 2.0 to 10.0. The obtained results (Fig. 7a) show that with the increasing pH, the anodic peak has moved towards more negative potentials. Figure 7b indicated a linear relation between potential and pH with a slope of approximately 0.059. According to the Nernst equation, it indicates the equal exchange of electrons and protons in this system. In part (c), the anodic peak currents were plotted versus pH; the maximum current was obtained

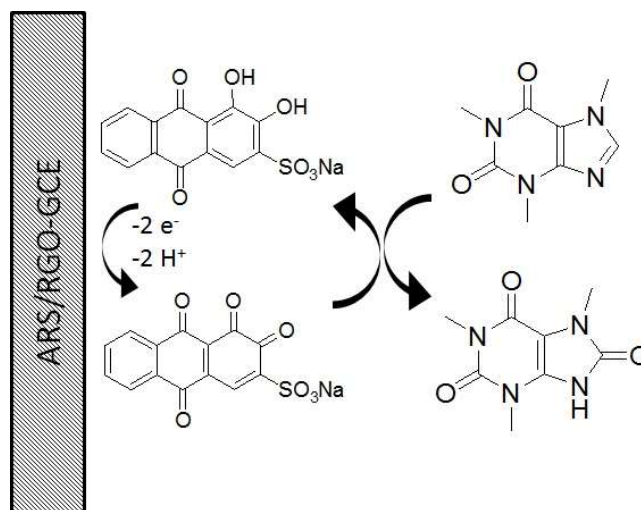


Fig. 6. Electrochemical oxidation mechanism of CAF on ARS/RGO-GCE *via* EC' mechanism.

at the pH of 4.0. Therefore, pH = 4.0 was chosen as the optimum pH in the following experiments.

Effect of Potential Scan Rate on Electrocatalytic Oxidation of Caffeine

Figure 8 shows the influence of potential scan rate on the CV responses of the ARS/RGO-GCE in the presence of $100 \mu\text{M}$ caffeine. With increasing the square root of the potential scan rate, the current of the anodic peak also increases linearly (Fig. 8a). It can be understood that the oxidation process of caffeine on the surface of the

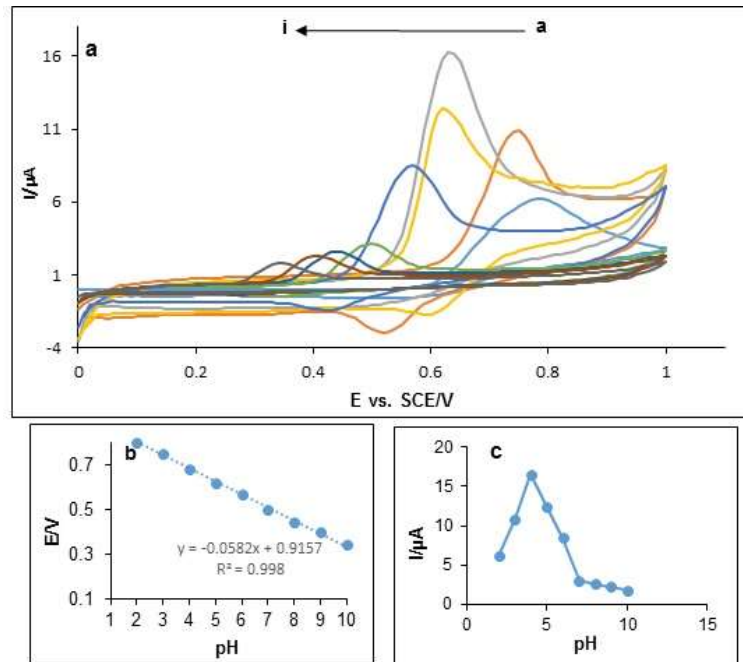


Fig. 7. (a) Cyclic voltammograms of the ARS/RGO-GCE in the presence of 100.0 μM caffeine with different pH in 0.1 M phosphate buffer solution (a \rightarrow i): 2.0, 3.0, 4.0, 5.0, 6.0, 7.0, 8.0, 9.0, 10.0; scan rate is 50 mV s^{-1} . Insets: plots of (b) E^o versus pH and (c) anodic peak current versus pH.

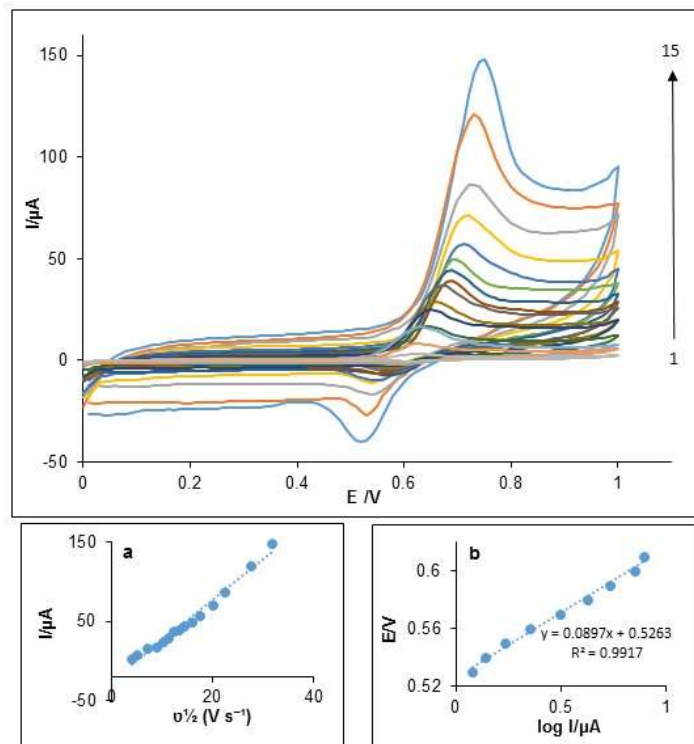


Fig. 8. Cyclic voltammograms of ARS/RGO-GCE in the presence of 100 M caffeine at different scan rates. Cycles 1-15 correspond to 15, 25, 50, 75, 100, 125, 150, 200, 250, 300, 400, 500, 750 and 1000 mV s^{-1} , respectively. insets: (a) the i_p versus $v^{1/2}$ (b) the Tafel curve (potential curve against the logarithm of the current intensity) of the Tafel region at the potential sweep rate 25 mV s^{-1} .

ARS/RGO-GCE is under diffusion control [25].

Figure 8b is the tafel curve that was drawn to obtain the value of the oxidative transfer coefficient. In this diagram, the Tafel region was used in the scanning speed of potential $0.25 \text{ s}^{-1} \text{ mV}$. Using the slope of the Tafel region and assuming that the number of electrons participating in the rate-determining step is 1.0, the value of the transfer coefficient in the oxidation of CAF at ARS/RGO-GCE was obtained 0.27.

Calibration Plot of Caffeine at the ARS/RGO-GCE

Because of the advantages of the differential pulse voltammetry (DPV) method in the quantitative analysis [43], this method was used for obtaining the calibration plot of CAF. In part (a) of Fig. 9, DPV voltammograms of ARS/RGO-GCE in 0.1 M solution of phosphate buffer with pH = 4.0 containing different concentrations of caffeine are displayed. In part (b) of this figure, the plot of peak current is drawn with respect to the concentrations of CAF. This graph is linear in the range of 1.0-100.0 μM of CAF concentration. By the slope of the calibration plot which is equal to 0.134 and the standard deviation of the blank solution ($s_b = 0.001 \mu\text{M}$), the detection limit of this electrochemical sensor for CAF was calculated as 0.022 μM .

Repeatability, Reproducibility, and Interference Studies

The repeatability and reproducibility are two important factors of a sensor for good analysis. For determining the repeatability of the sensor, the differential pulse

voltammograms of ARS/RGO-GCE were recorded three times in 0.1 M phosphate buffer solution with pH = 4.0 containing the same concentration of CAF (100.0 μM). The value of RSD for these measurements was obtained as %1.2. The interday and intraday measurements also were investigated. The RSD at 20, 50, and 100 μM of CAF were obtained as 2.3%, 2.1%, and 2.0% within a day (intraday precision, $n = 3$) and were found as 3.1%, 2.8%, and 2.5% within 5 days (interday precision, $n = 3$) confirmed the sensor had good repeatability [44].

To check the reproducibility of the sensor, the ARS/RGO-GCE was prepared independently three times, and each time the differential pulse voltammograms were recorded in 0.1 M phosphate buffer solution with pH = 4.0 and a certain amount of CAF (100.0 μM); the value of relative standard deviation was calculated as %1.84. Therefore, the repeatability and reproducibility of the proposed sensor are really excellent.

The effect of some interference species on the current response of oxidation of CAF was investigated. For this purpose, the DPV voltammograms of CAF with a concentration of 80.0 μM were recorded in the presence and absence of different concentrations of interfering species. The maximum concentration of species relative to CAF concentration that cannot disturb the CAF oxidation current more than 5% are obtained as glutamic acid (10 times), tryptophan (20 times), glycine (25 times), cysteine (30 times), and glucose (100 times).

Analysis of Real Samples

ARS/RGO-GCE can be used as an electrochemical sensor

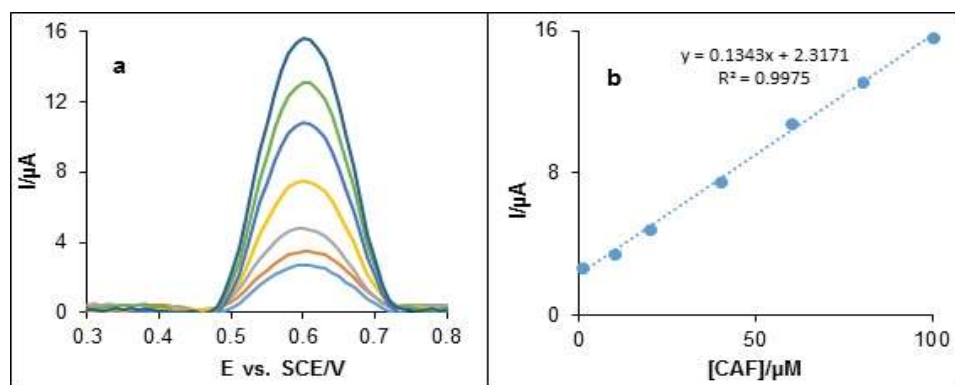


Fig. 9. (a) Differential pulse voltammograms of ARS/RGO-GCE in different concentrations of CAF (in order from bottom to top): 1.0, 10.0, 20.0, 40.0, 60.0, 80.0, and 100.0 μM ; (b) the plot of I_p versus CAF concentration.

Table 1. Analysis of CAF in some Real Samples by ARS/RGO-GCE and DPV Method (n = 3)

No.	Sample	CAF in the sample (μM)	Added CAF (μM)	Obtained CAF (μM) (Mean \pm SD)	Recovery percentage	Student 's t-test
1	Chocolate	3.7	26.3	30.7 \pm 0.9	102.66	1.35
2	milk	3.7	46.3	50.3 \pm 1.5	100.64	0.35
3	Black tea	17.5	12.5	29.5 \pm 1.0	99.2	0.87
4		17.5	32.5	49.9 \pm 2.1	99.69	0.08
5	Coffee	20.02	9.98	30.2 \pm 1.2	102	0.29
6	powder	20.02	29.98	50.5 \pm 1.9	101.6	0.46

to measure CAF concentration in different real samples. To investigate this ability, samples of black tea, coffee, and chocolate milk were used as real samples. A certain amount of these samples were added to 0.1 M phosphate buffer solution with pH = 4.0 and then a different amount of CAF was added to the samples. The solutions were analyzed by DPV at ARS/RGO-GCE. The results were calculated by standard addition method (each concentration was repeated three times) and the recovery percent was calculated. Table 1 shows the results. The results of the Student's t-test in various concentrations confirmed that no significant systematic error existed in our analysis based on a comparison of the obtained *t* value (last right column on Table 1) and critical *t* value (4.30 for three replicate measurements) [45].

CONCLUSIONS

In this research, a new sensing platform was developed based on ARS/RGO-GCE for the determination of CAF. The proposed sensor showed good electrocatalytic activity against CAF oxidation. The presence of RGO improved the properties of the electrochemical sensor due to unique properties such as high electron mobility, excellent electrical conductivity, and high surface area. ARS is also an electrochemically active species and was used in various types of electrochemical systems as an electron transfer mediator. But, in this work, instead of a simple combination of ARS and RGO, there was an interaction between them, and a composite of ARS/RGO was prepared and used in the construction of the electrode. The ARS/RGO obviously promoted the sensitivity of the oxidation of CAF. Also, a low detection limit (0.022 μM) was obtained by the modified electrode.

ACKNOWLEDGMENTS

The authors gratefully acknowledge Yazd University Research Council for their financial support.

REFERENCES

- [1] B.C. Gu, K.J. Chung, B.W. Chen, Y.H. Dai, C.C. Wu, *Electrochim. Acta* 463 (2023) 142820.
- [2] J. Zuo, W. Tang, Y. Xu, *Anti-hepatitis B virus activity of chlorogenic acid and its related compounds*, in: *Coffee in health and disease prevention*, Academic Press, 2015.
- [3] J. dePaula, A. Farah, *Beverages* 5 (2019) 37.
- [4] E. Dinç, A. Üçer, N. Ünal, *Food Chem.* 421 (2023) 136139.
- [5] A. Wong, A.M. Santos, M.H. Feitosa, O. Fatibello-Filho, F.C. Moraes, M.D. Sotomayor, *Biosensors* 13 (2023) 690.
- [6] A.K. Ghosh, C. Ghosh, A. Gupta, *Journal of agricultural and food chemistry* 61 (2013) 3814.
- [7] C. Du, C. Ma, J. Gu, L. Li, G. Chen, *Sensors* 20 (2020) 819.
- [8] J.Y. Sun, K.J. Huang, S.Y. Wei, Z.W. Wu, F.P. Ren, *Colloid. Surf. B* 84 (2011) 421.
- [9] M.S. El-Shahawi, A. Hamza, S.O. Bahaffi, A.A. Al-Sibai, T.N. Abduljabbar, *Food Chem.* 134 (2012) 2268.
- [10] A. Shishov, N. Volodina, D. Nechaeva, S. Gagarinova, A. Bulatov, *Microchem. J.* 144 (2019) 469.
- [11] A.D. Meinhart, C.S. Bizzotto, C.A. Ballus, M.A. Prado, R.E. Bruns, J. Teixeira Filho, H.T. RGOdoy, *Food Chem.* 120 (2010) 1155.

- [12] I.N. Pasiyas, I. Kiriakou, C. Proestos, *Antioxidants* 6 (2017) 67.
- [13] F.F. Al-Qaim, Z.H. Mussa, M.R. Othman, M.P. Abdullah, *J. Hazard. Mat.* 300 (2015) 387.
- [14] R. Rosal, A. Rodríguez, J.A. Perdigón-Melón, A. Petre, E. García-Calvo, M.J. Gómez, A. Agüera, A.R. Fernández-Alba, *Chemosphere* 74 6 (2009) 825.
- [15] A.G. Trovó, T.F. Silva, O. RGOmes Jr, A.E. Machado, W.B. Neto, P.S. Muller Jr, D. Daniel, *Chemosphere* 90 (2013) 170.
- [16] J.Y. Sun, K.J. Huang, S.Y. Wei, Z.W. Wu, F.P. Ren, *Colloid. Surf. B* 84 (2011) 421.
- [17] A. Wong, A.M. Santos, R. da Fonseca Alves, F.C. Vicentini, O. Fatibello-Filho, M.D.P.T. Sotomayor, *Talanta* 222 (2021) 121539.
- [18] J. Jose, V. Subramanian, S. Shaji, P.B. Sreeja, *Scientific Reports* 11 (2021) 11662.
- [19] M. Velmurugan, B. Thirumalraj, S.M. Chen, F.M. Al-Hemaid, M.A. Ali, M.S. Elshikh, *J. Colloid Interface Sci.* 485 (2017) 123.
- [20] L. aníková-Bandžuchová, R. Šelešovská, K. Schwarzová-Pecková, J. Chýlková, *Electrochim. Acta* 154 (2015) 421.
- [21] V. Hassanzadeh, M.A. Sheikh-Mohseni, B. Habibi, *J. Electroanal. Chem.* 847 (2019) 113200.
- [22] J.M. Zen, A. Senthil Kumar, D.M. Tsai, *Electroanalysis*, 15 (2003) 1073.
- [23] M. Mazloun-Ardakani, M.A. Sheikh-Mohseni, *Carbon Nanotubes in Electrochemical Sensors*, in: *Carbon Nanotubes-growth and Applications*, M. Naraghi (Ed.), InTech, Croatia, 2011.
- [24] M. Opallo, A. Lesniewski, *J. Electroanal. Chem.* 656 (2011) 2.
- [25] M. Mazloun-Ardakani, M.A. Sheikh-Mohseni, B.F. Mirjalili, *Ionics* 20 (2014) 431.
- [26] M.M. Barsan, M.E. Ghica, C.M. Brett *Anal. Chim. Acta* 881 (2015) 1.
- [27] M. Mazloun-Ardakani, M.A. Sheikh-Mohseni, B.F. Mirjalili, R. Ahmadi, M.A. Mirhoseini, *Chinese J. Catal.* 36 (2015) 1273.
- [28] S. Gentil, C. Pifferi, P. Rousselot-Pailley, T. Tron, O. Renaudet, A. Le RGOff, *Langmuir* 37 (2021) 1001.
- [29] J. Xu, Y. Wang, S. Hu, *Microchim. Acta* 184 (2017) 1.
- [30] A. Star, Y. Liu, K. Grant, L. Ridvan, J.F. Stoddart, D.W. Steuerman, J.R. Heath, *Macromolecules* 36 (2003) 553.
- [31] J.L. Stevens, A.Y. Huang, H. Peng, I.W. Chiang, V.N. Khabashesku, J.L. Margrave, *Nano Lett.* 3 (2003) 331.
- [32] R.J. Chen, Y. Zhang, D. Wang, H. Dai, *J. American Chem. Soc.* 123 (2001) 3838.
- [33] A.H. Mhemeed, *HIV Nursing* 22 (2022) 865.
- [34] M. Mazloun-Ardakani, M.A. Karimi, S.M. Mirdehghan, M.M. Zare, R. Mazidi, *Sens. Actuat. B Chem.* 132 (2008) 52.
- [35] M.A. Karimi, A. Hatefi-Mehrjardi, M. Mazloun-Ardakani, R. Behjatmanesh-Ardakani, M.H. Mashhadizadeh, S. Sargazi, *Inter. J. Electrochem. Sci.* 5 (2010) 1634.
- [36] K. Wu, S. Hu, *Carbon* 42 (2004) 3237.
- [37] J. Liu, D. Zhou, X. Liu, K. Wu, C. Wan, *Colloid. Surf. B Biointerfaces* 70 (2009) 20.
- [38] M. Mazloun-Ardakani, B. Barazesh, A. Khoshroo, M. Moshtaghiun, M.H. Sheikha, *Bioelectrochem.* 121 (2018) 38.
- [39] K.A. Mkhoyan, A.W. Contryman, J. Silcox, D.A. Stewart, G. Eda, C. Mattevi, M. Chhowalla, *Nano Lett.* 9 (2009) 1058.
- [40] T. Moriguchi, K. Yano, S. Nakagawa, F. Kaji, *J. Colloid Interface Sci.* 260 (2003) 19.
- [41] M. Sharp, M. Petersson, K. Edström, *J. Electroanal. Chem. Interface Electrochem.* 95 (1979) 123.
- [42] E. Laviron, *J. Electroanal. Chem. Interface. Electrochem.* 101 (1979) 19.
- [43] D.A. Skoog, F.J. Holler, T.A. Nieman, *Principles of Instrumental Analysis 5th edition*" Saunders College Pub. Co., Phila, 1998.
- [44] S.M. Khoshfetrat, I. Chegeni, *Sens. Actuators B: Chem.* 397 (2023) 134668.
- [45] S.M. Khoshfetrat, K. Fasihi, F. Moradnia, H.K. Zaidan, E. Sanchooli, *Anal. Chim. Acta* 1252 (2023) 341073.